CHEMISTRY OF MATERIALS
Article

Chem. Mater. **2009,** *21,* 5809–5818 5809
DOI:10.1021/cm902377p

Method for Large-Scale Production of Multimetallic Layered Double Hydroxides: Formation Mechanism Discernment

Jaime S. Valente,*[,†] Manuel Sánchez-Cantú,[‡] Enrique Lima,[§] and François Figueras[⊥]

[†]*Instituto Mexicano del Petróleo, Eje Central #152, 07730 Mexico, D. F., Mexico,* [‡]*BUAP, Facultad de Ingenieria Quimica, Avenida San Claudio y 18 Sur, 72570 Puebla, Puebla, Mexico,* [§]*UNAM, Instituto de Investigaciones en Materiales, Circuito exterior s/n CU, 04510 Mexico, D. F., Mexico, and* [⊥]*IRCE-LYON, UMR5256 CNRS-Universite LYON 1, 2 Avenue A. Einstein, 69626 Villeurbanne, France*

Received August 2, 2009. Revised Manuscript Received October 26, 2009

A simple, economical, and environmentally friendly method for the production of layered double hydroxides (LDHs) is presented. The synthesis procedure is based on dispersing insoluble metal oxides, adjusting the pH by adding an optimum amount of metal nitrates, and dispersing and aging the product for a short time (6−8 h). The final product does not require washing, opposite to the traditional coprecipitation synthesis procedure. A dissolution−precipitation−recrystallization mechanism is proposed for the formation of LDHs, based on particle size measurements, XRD analyses, radial distribution functions, and ^{27}Al MAS NMR studies. Solids were characterized by XRD, N_2 physisorption, TGA-DTA, SEM, and TEM, revealing that both LDHs and their calcination products have very similar properties to those prepared by conventional procedures. Pure LDH phase is obtained after 6−8 h; a large, uniform particle size that would usually require prolonged hydrothermal treatments is attained. Surface areas ranged from 32 to 93 $m^2\ g^{-1}$ and from 140 to 230 $m^2\ g^{-1}$ for fresh and calcined samples, respectively. This new method is intended to satisfy the growing demand of LDHs in large-scale applications as catalysts, SO_x adsorbents, PVC additives, etc.

Introduction

Layered double hydroxides (LDHs), also known as hydrotalcite-like compounds, are a group of naturally occurring anionic clays. Their structure resembles that of brucite, and is created by replacing a fraction of the divalent cations in the brucite lattice by trivalent cations, conferring a positive charge to the layers. The charge is electrically compensated by anions located in the interlayer region. An extensive family of compounds with LDH structure can be prepared, represented by the general formula: $[M^{2+}_{1-x}M^{3+}_{x}(OH)_2]^{x+}A^{z-}_{x/z}\cdot mH_2O$, where M^{2+} is a divalent cation (Mg^{2+}, Ni^{2+}, Zn^{2+}, Co^{2+}, Fe^{2+}, etc.), M^{3+} is a trivalent cation (Al^{3+}, Fe^{3+}, Cr^{3+}, etc.), and A^{z-} can be almost any organic or inorganic anion.[1]

LDHs are multipurpose materials that have found many applications, e.g., as sorbents, anion exchangers, drug delivery carriers, PVC additives, and fire retardants. Furthermore, they have been proposed as basic catalysts able to substitute liquid bases in many organic transformations.[2] LDHs have been recently studied as additives to trap sulfur oxides (SO_x) from the flue gases generated by fluid catalytic cracking units (FCC units), used to crack petroleum feedstocks.[3−6] They could also be used in coal-fired power plants and certain chemical manufacturing plants, where SO_x additives are also employed. These are all large scale applications, which require manufacturing LDHs at an industrial scale. Therefore, an economical and "green synthesis" method for large-scale production is of the utmost importance.

The most common method to prepare LDHs is by coprecipitation of metallic salts with a concentrated alkaline solution. Nevertheless, this method requires prolonged hydrothermal treatments that increase the cost of preparation. Besides, enormous amounts of water are required to wash the final products, in order to eliminate undesirable counterions such as K^+, Na^+, Cl^-, NO_3^-, etc. For instance, to prepare 1 ton of a MgAl LDH by coprecipitation, roughly 12 m^3 of water would be used for dissolution of the metal salts, plus 15 m^3 for the alkaline solution, and about 120 m^3 for washing the precipitate. Moreover, if nitrate salts were used as metal precursors and KOH-K_2CO_3 were used for the alkaline solution, waste waters would carry 1.7 ton of NO_3^-, 1.17 ton of K^+, and 0.60 ton of CO_3^{2-}. Special infrastructure would also be required for handling such large volumes of highly acidic and basic solutions.

Recent attempts at preparing LDHs on a large scale by an economical method have been presented in the

*To whom correspondence should be addressed. Phone: + 52 (55) 9175-8444. E-mail: jsanchez@imp.mx.

(1) Cavani, F.; Trifiro, F.; Vaccari, A. *Catal. Today* **1991**, *11*, 173.
(2) Figueras, F. *Top. Catal.* **2004**, *29*, 189.
(3) Zhuo, G. L.; Chen, Y. F.; Ge, Z. H.; Jiang, X. Z. *Chin. Chem. Lett.* **2002**, *13*, 279.
(4) Polato, C. M. S.; Henriques, C. A.; Neto, A. A.; Monteiro, J. L. F. *J. Mol. Catal. A* **2005**, *241*, 184.
(5) Andersson, P-O. F.; Pirjamali, M.; Järås, S. G.; Boutonnet-Kizling, M. *Catal. Today* **1999**, *53*, 565.
(6) Cantu, M.; Lopez-Salinas, E.; Valente, J. S.; Montiel, R. *Environ. Sci. Technol.* **2005**, *39*, 9715.

Published on Web 11/13/2009

scientific and patent literature.[7−20] For instance, continuous production of LDHs by an in-line dispersion−precipitation method was reported.[13] However, it employs an alkaline solution to precipitate the metallic salts; thus, the purification and handling problems are not avoided. Another approach was the preparation of LDHs using metal oxides/hydroxides, but it required long aging times and the final products contained, among other phases, brucite, gibbsite, and boehmite.[7,14,15] A method slightly resembling the one here presented has been patented.[16−18] Nevertheless, prolonged aging times were usually necessary, and in some cases, relatively pure compounds were obtained only after hydrothermal treatment. Moreover, to avoid the presence of unreacted precursors and secondary crystalline phases, the pH was necessarily adjusted using an acid (HNO_3, HCOOH) or a base (NH_4OH, NaOH). Another method used MgO and activated alumina to obtain meixnerite, which is then contacted with a polyvalent inorganic anion, to produce an LDH.[19] Furthermore, a procedure that uses an aluminum-containing compound and a magnesium-containing compound to obtain an amorphous precipitate, which is then heat-treated and rehydrated to obtain an LDH, used for SO_x removal, has been patented.[20] All the aforementioned methods are limited to the preparation of bimetallic LDHs, mainly MgAl. Additionally, the LDH formation mechanisms have yet to be elucidated. Other differences and advantages of the method here presented have been reviewed previously.[21]

The authors have reported a promising method to prepare multimetallic LDHs at large scale, under environmentally friendly conditions, and advantageous from an economical view.[21,22] The raw materials in this preparation are insoluble oxides, and the method is based on dissociation, hydrolysis, and peptization reactions. LDHs are obtained under mild conditions and short synthesis times, using a minimal amount of water. However, the mechanism of LDHs formation by this method still remains unclear. The aggregation of the different species formed during the evolution from insoluble oxides to LDHs should be understood, in order to explain the physicochemical properties of materials prepared through this method. Thus, this work is devoted to describe in detail the structural and textural properties of the LDHs synthesized by this new method.

Scheme 1. Synthesis Steps for LDH Formation

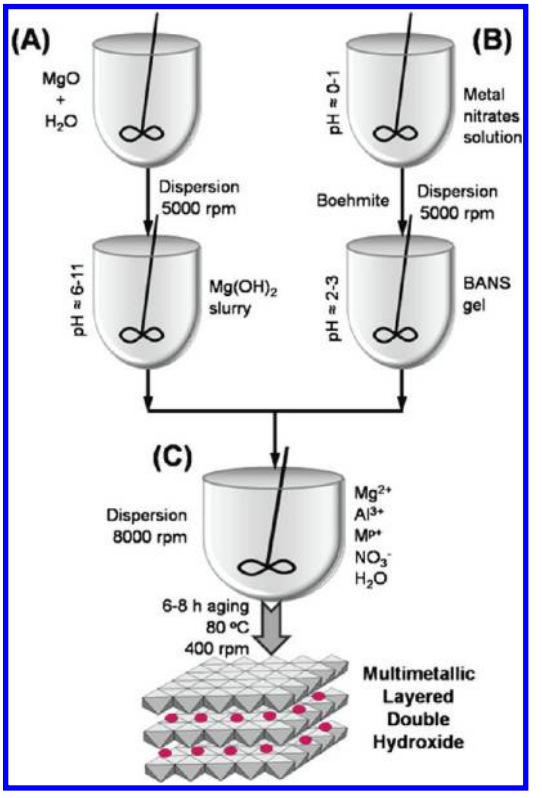

Experimental Details

Synthesis Procedure. Technical-grade MgO and Boehmite purchased from Peñoles and Engelhard were used as magnesium and aluminum sources, respectively. Chemical compositions of both sources were measured by X-ray Spectrometry, in order to determine their metal content. The general synthesis steps of multimetallic LDHs, $MgM^{p+}Al$, where M^{p+} = Mg^{2+}, Ni^{2+}, Cu^{2+}, Zn^{2+}, Al^{3+}, and Fe^{3+}, were performed as follows (Scheme 1): MgO was dispersed in water at 5000 rpm (A). In parallel, M^{2+} and/or M^{3+} nitrates were dissolved. Afterward, enough boehmite was added to achieve the desired M^{2+}/M^{3+} molar ratio and the mixture was dispersed at 5000 rpm (B). The H_2O/solid weight ratio was 10. Thereafter, the product resulting from the addition of (A) to (B) was dispersed at 8000 rpm (C). The slurry was aged at 80 °C for 6−8 h with a stirring speed of 400 rpm. Finally, the solid was filtered and dried at 100 °C for 12 h. For the detailed synthesis procedure of each compound, see the Supporting Information.

Characterization Techniques. Dispersions of the metallic oxides were performed with an ultraturrax T-50 from IKA (speed range from 4000 to 10000 rpm) with a S50N-G45G dispersion attachment. Particle size measurements were performed on an HORIBA equipment model LA-500 by the ASTM D-4464 method. A 0.2% solution of sodium hexaphosphate was used as dispersing media. Prior to analysis, the samples were dispersed with ultrasound equipment for 3 min. Chemical composition was determined in a Siemens X-ray spectrometer SRS 3000. Powder X-ray diffraction patterns were obtained in a Siemens D-5000 with Cu Kα radiation operating at 35 kV and 25 mA. Data were collected in the 2θ range from 4 to 70° with 0.02° step size and a counting time of 0.6 s/point. The radial

(7) Xu, Z. P.; Lu, G. Q. *Chem. Mater.* **2005**, *17*, 1055.
(8) Kelkar, C. P.; Schutz, A. A. *Microporous Mater.* **1997**, *10*, 163.
(9) Thomas, G. S.; Kamath, P. V. *Mater. Res. Bull.* **2002**, *37*, 705.
(10) Newman, S. P.; Jones, W.; O'Connor, P.; Stamires, D. *J. Mater. Chem.* **2002**, *12*, 153.
(11) d' Espninose, J.-B.; Kermarec, M.; Clause, O. *J. Am. Chem. Soc.* **1995**, *117*, 11471.
(12) Rajamathi, M.; Kamath, P. V. *Bull. Mater. Sci.* **2000**, *23*, 355.
(13) Abelló, S.; Pérez-Ramírez *J. Adv. Mater.* **2006**, *18*, 2436.
(14) Turner, R. C.; Brydon, J. E. *Science* **1962**, *136*, 1052.
(15) Mascolo, G.; Marino, O. *Miner. Mag.* **1980**, *43*, 619.
(16) Jones, W.; Stamires, D.; Brady, M. U. S. Patent 6,541,409, **2003**.
(17) Stamires, D.; Jones, W. U. S. Patent 6 440 888, **2002**.
(18) Stamires, D.; O'Connor, P.; Jones, W.; Brady, M. U. S. Patent 6 800 578, **2004**.
(19) Martin, E. S.; Stinson, J. M.; Cedro, V., III; Horn, W. E., Jr. U. S. Patent 5 730 951, **1998**.
(20) Vierheilig, A. A. U. S. Patent 6 028 023, **2000**.
(21) Sanchez-Valente, J.; Lopez-Salinas, E.; Sanchez-Cantu, M. U. S. Patent 2008/027034 A1, **2008**.
(22) Valente, J. S.; Cantu, M. S.; Figueras, F. *Chem. Mater.* **2008**, *20*, 1230.

distribution functions (RDFs) were calculated from the full diffraction patterns as shown by Magini and Cabrini.[23] In order to reach the required high values of the angular parameter $h = (4\pi\sin\theta)/\lambda$, a molybdenum anode X-ray tube was used and the X-ray pattern was measured by step scanning at angular intervals of 0.02°. ^{27}Al MAS NMR spectra were acquired on a Bruker Avance II spectrometer, with a magnetic field strength of 7.05 T, corresponding to a ^{27}Al Larmor frequency of 78.3 MHz. Samples were packed in ZrO_2 rotors and they were spun at 10 kHz. Short single pulses ($\pi/12$) with a repetition time of 0.5 s were used. Chemical shifts were referenced to an aqueous 1N $AlCl_3$ solution. Thermogravimetric analyses were carried out using Perkin-Elmer TG-7. Samples were heated in flowing dry air (20 mL min^{-1}) from room temperature to 1000 °C, with a constant heating rate of 10 °C min^{-1}. Surface areas, pore volume and pore size distribution of the calcined samples were obtained from the N_2 physisorption isotherms determined at −196 °C on a Quantachrome Autosorb-1C equipment. Surface areas were calculated by using BET equation and pore size distributions were calculated by the BJH method using the desorption branch. Prior to N_2 adsorption, fresh and calcined samples were outgassed at 100 and 350 °C overnight, respectively. Scanning Electron Microscopy (SEM) was performed in a Philips ESEM XL30 with an acceleration voltage of 25 kV and a NOVA 200 Nanolab operating at 30 kV. Chemical composition of the particles was determined by EDS (energy-dispersive spectrometry). Prior to the measurements with the NOVA 200 the samples were covered with gold and mounted on a carbon film. Transmission Electron Microscopy (TEM) images were acquired in a JEOL JEM 2200 FS operating at an acceleration voltage of 200 kV. Prior to analysis, the samples were mounted on a copper grid coated with a carbon film.

Results and Discussion

Dispersion and Formation Studies. *Magnesium−Aluminum LDH.* The particle size distribution after mechanical dispersion was studied, in order to find the optimal time and speed parameters to obtain a pure LDH phase. The study consisted in dispersing in water, at a fixed rate for distinct periods, the pristine MgO and the mixture of boehmite with the aluminum nitrate solution, respectively. Figure 1 shows the particle size distribution resulting from the mechanical dispersion of the precursors and the reaction mixture.

MgO powder (Figure 1A) exhibited a uniform particle size distribution between 1 and 20 μm with an average size of 5.39 μm (Supporting Information). After stirring at 300 rpm for 10 min the average size increased to 7.11 μm, which was attributed to the formation of $Mg(OH)_2$ from MgO hydration. This supposition was confirmed by XRD analysis (Figure 2). When dispersing MgO for 15, 30, and 60 min at 5000 rpm, the average particle sizes were 5.39, 3.59, and 3.51 μm, with uniform distributions between 0.65 and 20, 0.4−16 and 0.2−16 μm, respectively. An aliquot was taken for the sample dispersed for 30 min and characterized by XRD (Figure 2). The result confirms once again the total conversion of MgO into $Mg(OH)_2$, which showed a crystal size of 131 Å (calculated from the (101) plane), very similar to that obtained for MgO without dispersion (133 Å).

The same study was applied to the boehmite-aluminum nitrate solution (BANS), Figure 1B. Boehmite powder had a broad distribution between 1 and 200 μm and an average particle size of 24.56 μm. A gel was formed when

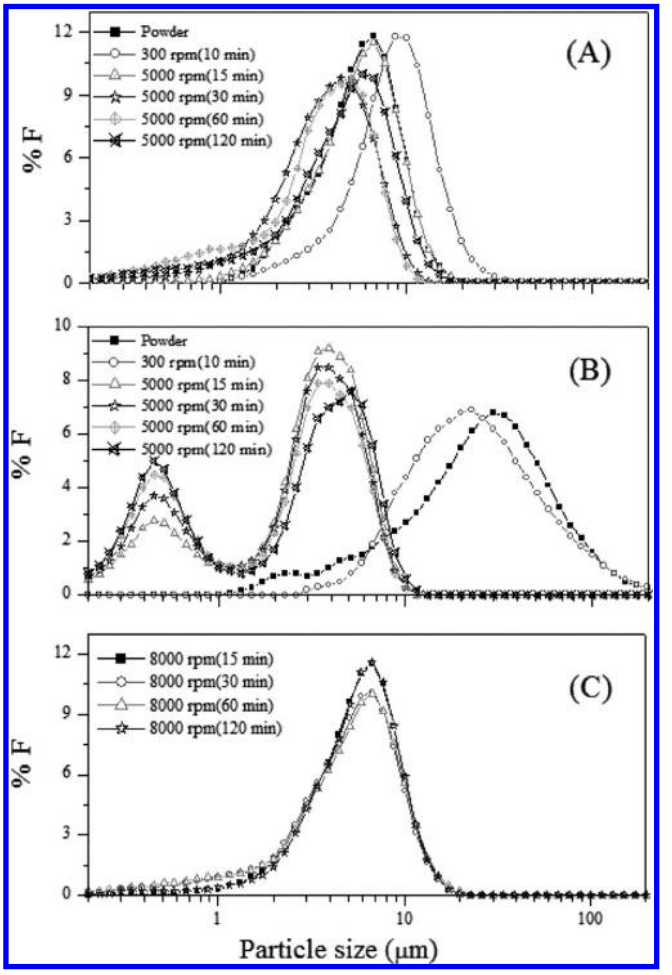

Figure 1. Particle size distribution resulting from the dispersion of (A) MgO, (B) boehmite-aluminum nitrate solution, and (C) reaction mixture of (A) and (B).

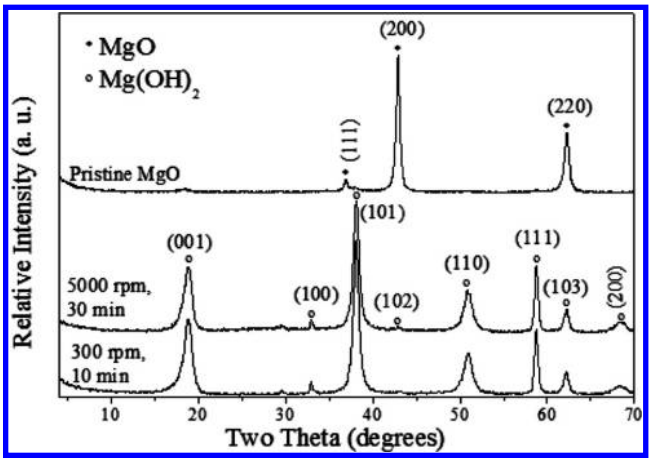

Figure 2. X-ray patterns of pristine MgO, after agitation at 300 rpm for 10 min, and dispersion for 30 min at 5000 rpm, respectively. Samples were taken from the mother liquor, filtered to eliminate the excess of water, and analyzed without further treatment.

(23) Magini, M.; Cabrini, A. *J. Appl. Crystallogr.* **1972**, *5*, 14.

the boehmite powder was added to the aluminum nitrate solution; this gel had an average particle size of 21.18 μm with a particle size distribution between 2.5 and 200 μm. When dispersing the gel for 15, 30, 60, and 120 min, a considerable size decrease (3.01, 2.78, 2.60, and 2.75 μm, respectively) was observed; particles had a bimodal size distribution, centered at ~0.4 and ~4 μm.

A portion of this gel, agitated for 10 min at 300 rpm, and of that dispersed for 15 min at 5000 rpm was filtered and analyzed by X-ray diffraction (Supporting Information). Only boehmite phase was detected; signals were broadened because of the high amounts of water present in the samples.[24] Crystal sizes, calculated from the (020) plane for the boehmite powder, the sample agitated at 300 rpm, and the one dispersed at 5000 rpm were 28, 21, and 18 Å, respectively.

It is worth noticing that crystal sizes did not suffer any significant modification in any case. The main variations were in the average particle sizes, especially in the BANS gel. Decreasing the particle size of the precursors, and of those particles present in the reaction mixture, leads to an increment of available particles and reactive surfaces. This allowed for obtaining pure crystalline phases in shorter reaction times.

Dispersion for 30 min was selected as the optimum time for both MgO and BANS. In MgO, as can be observed in Figure 1A, particle size did not decrease after 30 min; on the contrary, after 120 min it began to increase. In BANS, Figure 1B, the bimodal distribution does not change with time, but the relative proportion of smaller particles increases continuously. Here, a 30 min dispersion time was considered sufficient and was chosen mainly for economy; it must be kept in mind that, for an industrial process, time has an important effect on production costs.

When the MgO dispersion was added to the BANS gel, the dispersion rate was increased from 5000 to 8000 rpm because of the slurry's viscosity increase. A homogeneous distribution (between 0.2 and 20 μm) was obtained for dispersions at 15, 30, 60, and 120 min (average particle sizes of 5.36, 4.95, 5.04, and 5.39 μm, respectively, Figure 1C). In this case, a dispersion time of 60 min was chosen, given the achieved particle sizes and the final appearance of the slurry. It is worth mentioning that when dispersing the mixture of MgO and BANS at 8000 rpm, mechanic energy induced a temperature increase, reaching 70 °C after 120 min. This was considered beneficial, because this initial thermal treatment could facilitate obtaining a pure crystalline phase in shorter reaction times. Mechanical dispersion has been also employed by other authors for the synthesis of the anionic clays;[13] however, they synthesized their compounds by the typical coprecipitation method.

Once the dispersion conditions were established, the slurry was allowed to cool to room temperature and agitated for 10 min at 400 rpm, and a first aliquot was taken. The slurry was then placed in a batch reactor, the

(24) Jenkins, R.; Snyder, R. L. *Introduction to X-ray Powder Diffractometry*; John Wiley and Sons: New York, 1996; Chapter 2, pp 138−215.

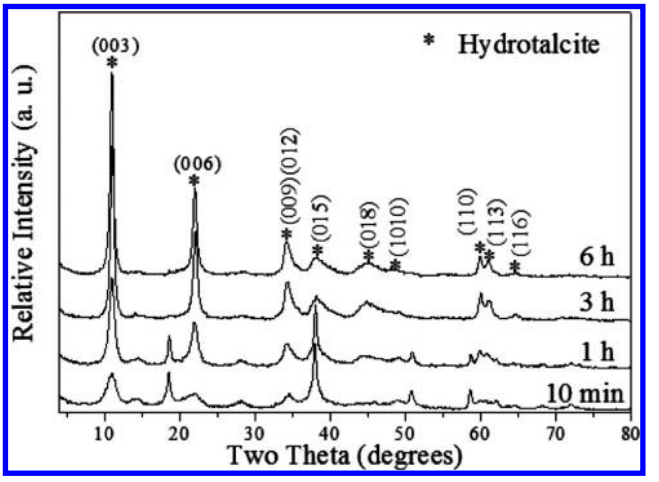

Figure 3. Powder XRD patterns of the MgAl LDH's evolution.

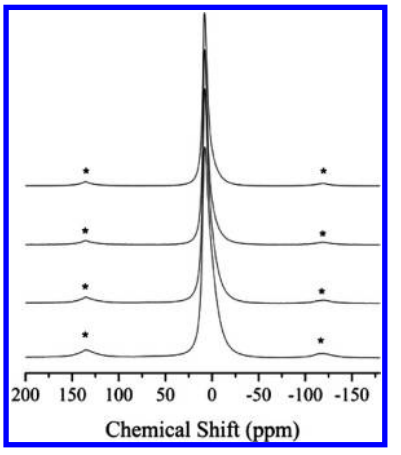

Figure 4. ^{27}Al MAS NMR spectra of MgAl LDH at different synthesis times. From bottom to top, samples aged for 10 min and 1, 3, and 6 h.

temperature was increased to 80 °C, and aliquots were taken at 1, 3, and 6 h. The reaction's evolution was monitored by XRD, showing the precursor's disappearance from the final dispersed slurry (Figure 3). The sample agitated for 10 min consisted in a mixture of brucite, boehmite and LDH phases. After aging for 1 h, boehmite and brucite reflections diminished substantially, and at 3 h, they almost disappeared. No boehmite could be detected after 6 h. It is worth noting that the solids were not washed at any of the synthesis steps.

Figure 4 displays the ^{27}Al MAS NMR of samples at 10 min, and 1, 3, and 6 h. Samples presented only one isotropic peak close to 5 ppm, which is due to aluminum 6-fold coordinated to oxygen atoms. Whereas no significant differences were observed concerning the peak's position, it became narrower with time (see the Supporting Information). This result confirms the XRD observations regarding the progressive aggregation of octahedral aluminum species to a matrix composed by octahedral aluminum and magnesium, i.e., into the LDH framework.

The broadest line at 10 min is due to initial aluminum species in aluminum hydroxide particles, as proposed later in the reaction mechanism. Here, the number of

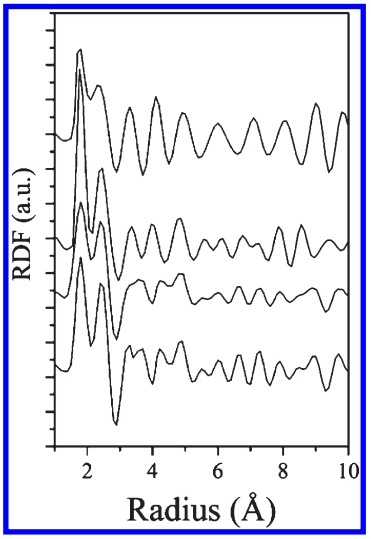

Figure 5. Radial distribution functions of MgAl LDH at different synthesis time. From bottom to top, samples aged for 10 min and 1, 3, and 6 h.

aluminum−aluminum pairs is maximal. With the formation of LDH layers, many of the Al−Al pairs disappeared, and Al−Mg pairs, bridged by oxygen atoms, emerged.

Radial distribution functions (RDF) are presented in Figure 5. The peaks, due to Al−Al and Mg−Mg distances, were clearly resolved at 3.67 and 3.19 Å, respectively, for sample taken at 10 min. With time, these two peaks fade out, and a broader peak appears centered at 3.31 Å, which can be assigned to Mg−Al distance. It seems, then, that under these conditions a core of magnesium hydroxide was first formed, and afterward aggregation−diffusion of aluminum lead to LDH formation. Mg−O and Al−O distances were unresolved, appearing both enclosed in a peak located at 1.7 Å (first neighbors) and at 4.21 Å (second neighbors). With time, the peak at 1.7 Å remains unaltered, as expected. However, the peak at 4.21 Å disappears, because the incorporation of aluminum into the LDH lattice leads to new distances Al−O, Mg−O, and O−O (dependent on the O−Me−O bond angle), which are together in a broad peak centered at 4.05 Å. Besides, the short- and long-range order is maintained for samples taken after 10 min. On the contrary, for synthesis times as long as 3 h, the long-range order is lost, as shown by the broadness of the peaks.

These observations should be understood as a slow diffusion of aluminum into the LDH framework. This result shows the versatility of this method, because synthesis time can be adjusted to obtain composite materials, with a core enriched in magnesium and an outer shell enriched in aluminum. The LDH formation from these sources can be explained in terms of a dissolution−precipitation−recrystallization mechanism (vide infra).

Multimetallic LDHs. Multimetallic LDHs $MgM^{p+}Al$ containing a nominal 5% weight of M^{p+}, where M^{p+} = Ni^{2+}, Cu^{2+}, Zn^{2+}, and Fe^{3+} were synthesized. In some cases, dispersion times were modified in order to obtain pure phases; times and stirring speeds were based on the XRD patterns of the final products. As shown in Figure 6,

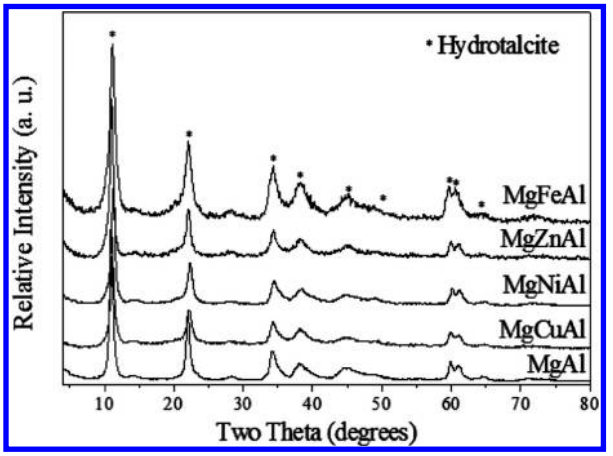

Figure 6. Powder X-ray diffraction patterns of the multimetallic LDHs.

all samples showed the characteristic reflections of the LDH phase.

Although only NO_3^- ions were introduced from metallic salts, the presence of carbonate anions trapped from the ambient cannot be discarded, since no special precautions were taken during the synthesis of the materials. According to Xu and Zeng,[25] the interlayer expansion, higher than the usually reported (23.2 Å), can be attributed mainly to an orientation change from the flat-lying to the stick-lying orientation of the nitrate ion.

Cell parameters c and a, and crystal sizes L_{003} and L_{110} were calculated from the principal reflections of the (003) and (110) planes, respectively (Table 1). The examination of the a parameter, which reflects the average cation−cation distance inside the brucite-like layers, is a simple way of analyzing the isomorphic substitution of Mg^{2+} or Al^{3+} by the M^{p+} cation.

The a values increased in the following order: MgNiAl < MgCuAl < MgZnAl < MgFeAl (from 3.077 to 3.101 Å for the MgNiAl and MgFeAl, respectively), which is in good agreement with the ionic radii of the M^{p+} cations. The inverse trend was noticed when the crystal size L_{003} was calculated, being MgFeAl < MgZnAl < MgCuAl < MgNiAl, whereas no tendency was found when the L_{110} was determined.

^{27}Al NMR spectra of multimetallic LDHs (Figure 7A) confirm the introduction of various metals into the LDH lattice. Only aluminum octahedrally coordinated is observed in all samples. The paramagnetic character of Fe^{3+} (electronic configuration [Ar] $3d^5$) and Ni^{2+} (electronic configuration [Ar] $3d^8$), also in octahedral coordination, created anisotropic tensors.

The chemical composition of all samples is presented in Table 1. The established nominal M^{2+}/M^{3+} molar ratio was 2.8; the actual ratio (determined by X-ray fluorescence) varied from 2.56 to 3.06, which is within experimental error.

Figure 8 exhibits the powder XRD patterns of the samples calcined at 500 °C. It has been demonstrated by XRD analyses that during calcination the layered

(25) Xu, Z. P.; Zeng, H. C. *J. Phys. Chem. B* **2001**, *105*, 1743.

Table 1. Chemical Composition, Cell Parameters, and Crystal Sizes of LDHs, and Their Calcination Products

sample	chemical formulas	M^{2+}/M^{3+}	a (Å)[a]	c (Å)[a]	L_{003} (Å)[a]	L_{110} (Å)[a]	a (Å)[b]	L_{200} (Å)[b]
MgAl	$[Mg_{0.754}Al_{0.246}\ OH)_2](NO_3)_{0.246}\ 0.64H_2O$	3.06	3.087	24.123	162	249	4.201	62
MgCuAl	$[Mg_{0.708}Cu_{0.051}Al_{0.241}(OH)_2](NO_3)_{0.241}\cdot 0.50H_2O$	2.73	3.085	23.787	149	196	4.196	62
MgNiAl	$[Mg_{0.662}Ni_{0.074}Al_{0.264}(OH)_2](NO_3)_{0.264}\cdot 0.60H_2O$	2.79	3.077	23.561	177	233	4.190	58
MgZnAl	$[Mg_{0.676}Zn_{0.068}Al_{0.256}(OH)_2](NO_3)_{0.256}\cdot 0.54H_2O$	2.91	3.088	24.010	130	232	4.196	63
MgFeAl	$[Mg_{0.756}Fe_{0.064}Al_{0.180}(OH)_2](NO_3)_{0.244}\cdot 0.59H_2O$	2.56	3.101	23.787	82	206	4.204	60

[a] Samples dried at 100 °C. [b] Samples calcined at 500 °C for 4 h, parameter determined for MgO phase.

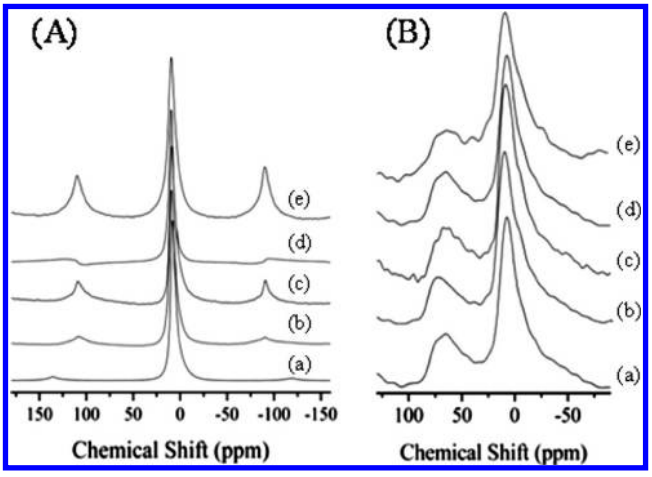

Figure 7. ^{27}Al MAS NMR spectra of multimetallic LDHs: (a) MgAl, (b) MgCuAl, (c) MgNiAl, (d) MgZnAl, and (e) MgFeAl. (A) fresh samples, (B) calcined (500 °C) samples.

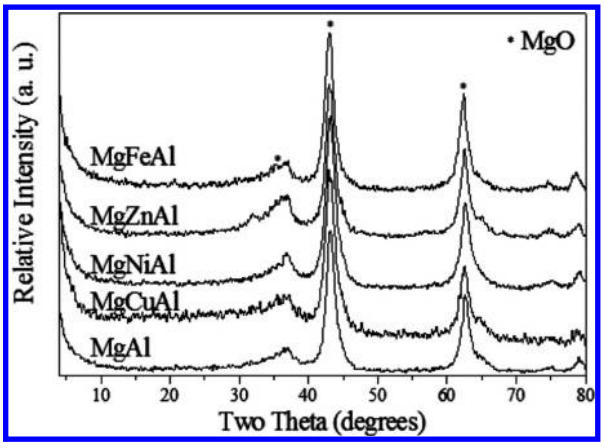

Figure 8. Powder XRD patterns of samples calcined at 500 °C.

structure collapses, obtaining an amorphous solid around 360 °C, that at approximately 400 °C crystallizes in a MgO-like phase. If the solid remains calcined below 800 °C, only the metal oxide of the metallic cation present in larger amount will be detected.[26,27] As expected, the main crystalline phase in all ternary LDHs was MgO (JCPDS file 04−0829) indicating that the other cations are highly dispersed in the MgO matrix, which is of great importance for their application, for instance as catalysts.[28]

The lattice parameters of the MgO-like structure obtained at 500 °C (Table 1) are lower than that of the pure MgO (4.213 Å), indicating that Al^{3+} and M^{p+} ions are dissolved in the lattice to form a solid solution. Thus, a relationship between the lattice parameter and the ionic radii of the M^{p+} can be observed being MgFeAl > MgZnAl ≈ MgCuAl > MgAl ≈ MgNiAl.

It is worth noting that even if the fresh samples presented distinct crystal sizes, the crystal sizes of the calcined solids calculated from the (200) reflection were very similar (between 58 and 64 Å), showing that the crystal size of the pristine LDH has no effect over the calcined material. Moreover, this indicates that the amount of defects in the MgO lattice should also be similar. Therefore, the quantity of basic sites should be comparable, according to the model proposed by Coluccia and Tench for the creation of basic sites.[29] In consequence, the basic strength will depend mainly on the chemical composition and the molar ratio M^{2+}/M^{3+}, and not on the defects generated through calcination.

In this sense, ^{27}Al NMR spectra of calcined samples (Figure 7B) reveal that the Al^{IV}/Al^{VI} ratio is close for all samples. However, because of the complex and heterogeneous composition of these samples, it cannot be established that all samples have the same acidity.

Proposed Mechanism for LDH Formation. A general LDH formation mechanism that was previously proposed[22] is shown in Scheme 1. Taking into account that when MgO was dispersed, it was completely hydrated into $Mg(OH)_2$, it can be supposed that when a divalent oxide is dispersed in water it will transform into its corresponding hydroxide through the following reaction

$$MO + H_2O \rightarrow M(OH)_2 \qquad (1)$$

A pH between 6 and 11 is achieved, according to the nature of the hydroxide.[30,31] This reaction is exemplified in section A of the reaction mechanism (Scheme 1).

According to the results presented here, the average particle size can be adjusted by the dispersion of the metallic oxide. On the other hand, in part B, by dissolving metallic nitrates and adjusting their concentration, the

(26) Millange, F.; Walton, R. I.; O'Hare, D. *J. Mater. Chem.* **2000**, *10*, 1713.
(27) Kanezaki, E. *Solid State Ionics* **1998**, *106*, 279.
(28) Sanchez-Valente, J.; Figueras, F.; Gravelle, M.; Kumbhar, P.; Lopez, J.; Besse, J.-P. *J. Catal.* **2000**, *189*, 370.
(29) Coluccia, S.; Tench, A. J. *Proceedings of the 7th International Congress on Catalysis*; Tokyo, June 30−July 4, 1980; Kodanaha: Tokyo, 1981; p 1160.
(30) Stumm, W.; Morgan, J. J. *Aquatic Chemistry: An Introduction Emphasizing Chemical Equilibria in Natural Waters*; John Wiley & Sons: New York, 1981; Chapter 5, pp 230−285.
(31) Baes, C. F.; Mesmer, R. E. *The Hydrolysis of Cations*, reprint ed.; Wiley: New York, 1986; Chapter 5, pp 95−98.

pH was regulated, giving an adequate acidic media for incorporating an insoluble metallic source such as boehmite. The effect of the mechanical dispersion was evidenced in the gel obtained from the mixture of the metallic nitrates with boehmite, achieving an average particle size ca. 9 times less than that of the pristine powder (Supporting Information). The reaction that exemplifies this step is the following

$$2\mathrm{AlOOH(s)} + 2\mathrm{H^+} \leftrightarrow 2\mathrm{Al^{3+}} + 2\mathrm{H_2O} \qquad (2)$$

Step C (Scheme 1) illustrates the addition of the suspension obtained from the hydrolysis of the metallic oxide represented by $M(OH)_2$ (A), the gel in B, and their dispersion for an optimal time. The time will depend on several factors such as the chemical composition, nature of the metallic precursors, and the system's pH. Such dispersion will facilitate the intimate contact between the metallic sources, creating a high population of nucleation centers that, together with the energy addition caused by the mechanical dispersion and the pH, will cause a change in the system's metastability,[32,33] which will initiate the formation of the LDH as the most stable crystalline phase.

The general proposed reactions for the formation of multimetallic LDHs are given in the following equations

$$(1-x)\mathrm{M(OH)(s)} + x[\mathrm{M}^{p+}(\mathrm{OH})_p(\mathrm{s})] + \left(\frac{x}{n}\right)\mathrm{A}^{n-} + m\mathrm{H_2O} \leftrightarrow [\mathrm{M}^{2+}_{(1-x)}\mathrm{M}^{3+}_{x}(\mathrm{OH})_2]\mathrm{A}^{n-}_{x/n}\cdot m\mathrm{H_2O} \qquad (3)$$

$$(1-x)\mathrm{M(OH)_2(s)} + x[\mathrm{M}^{p+}(\mathrm{OH})_4^{y-}] + \left(\frac{x}{n}\right)\mathrm{A}^{n-} + m\mathrm{H_2O} \leftrightarrow [\mathrm{M}^{2+}_{(1-x)}\mathrm{M}^{3+}_{x}(\mathrm{OH})_2]\mathrm{A}^{n-}_{x/n}\cdot m\mathrm{H_2O} \qquad (4)$$

$$(1-x)\mathrm{M}^{2+} + x[\mathrm{M}^{p+}(\mathrm{OH})_{\mathrm{p}(s)}] + \left(\frac{x}{n}\right)\mathrm{A}^{n-} + 2\mathrm{OH}^- + m\mathrm{H_2O} \leftrightarrow [\mathrm{M}^{2+}_{(1-x)}\mathrm{M}^{3+}_{x}(\mathrm{OH})_2]\mathrm{A}^{n-}_{x/n}\cdot m\mathrm{H_2O} \qquad (5)$$

$$(1-x)\mathrm{M}^{2+} + x[\mathrm{M}^{p+}(\mathrm{OH})_4^{y-}] + \left(\frac{x}{n}\right)\mathrm{A}^{n-} + 2\mathrm{OH}^- + m\mathrm{H_2O} \leftrightarrow [\mathrm{M}^{2+}_{(1-x)}\mathrm{M}^{3+}_{x}(\mathrm{OH})_2]\mathrm{A}^{n-}_{x/n}\cdot m\mathrm{H_2O} \qquad (6)$$

M^{2+} represents one, two, or more divalent metallic cations including Mg^{2+}, Cu^{2+}, Ni^{2+} and Zn^{2+}; M^{p+} refers to a combination of one or more M^{2+} and/or M^{3+} cations (where M^{3+} is Al^{3+} or Fe^{3+}). The $M^{p+}(OH)_4^{y-}$ is the ionic species found in basic media, for instance when $p = 2$, $y = 2$, and when $p = 3$, $y = 1$, respectively.[31] A^{n-} is the anion located in the interlayer region, with $n-$ being its electronic charge, and m corresponds to the hydration water molecules.

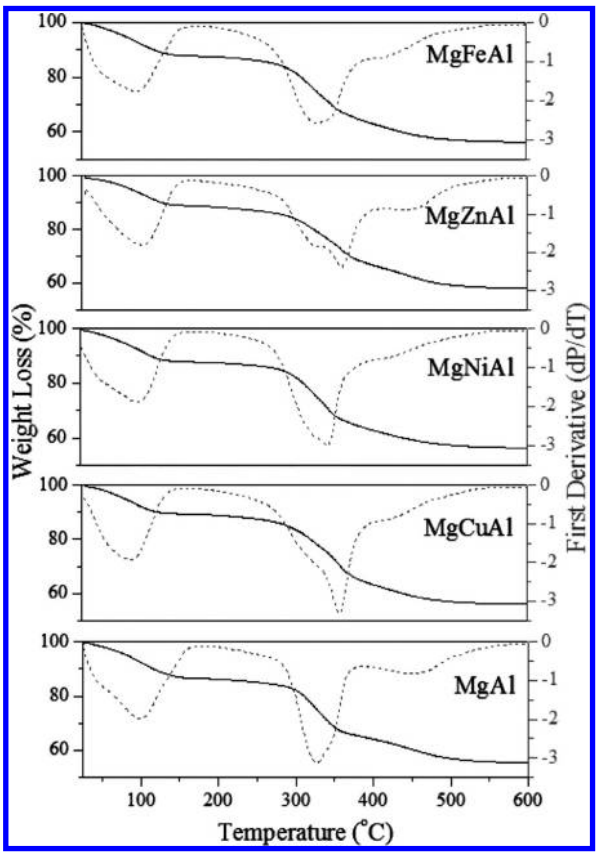

Figure 9. Thermogravimetric analyses of multimetallic LDHs.

According to the results presented above, it is considered that reaction 3 occurs immediately after mixing A and B. Depending on the nature of M^{p+}, the corresponding hydroxide $M^{p+}(OH)_p(s)$ will be formed either in acidic medium, as in the cases of the iron and aluminum hydroxides, or in neutral-basic medium for the copper, nickel, zinc, or magnesium ones.

As the solid-state reaction proceeds and the reaction media becomes progressively alkaline, the $M^{p+}(OH)_4^{y-}$ will be formed because of the dissociation of the corresponding hydroxides. In this step, control of pH is crucial to facilitate the dissociation of the bimetallic hydroxide $M(OH)_2(s)$. After dispersion in step C, pH values between 8 and 10 were obtained. It is worth mentioning that these pH values are commonly found during layered double hydroxide synthesis.[1] Therefore, it is assumed that reactions 4−6 were involved during the LDH formation. From these results we can conclude that dissolution−precipitation−recrystallization mechanisms are implicated throughout the preparation of the LDH compounds.

Thermal Decomposition. Figure 9 presents the thermogravimetric analysis results. It can be observed that the thermogravimetric (TG) curves are very similar, showing four weight loss steps. The total weight loss percentages oscillated between 42 and 45%. To show evidence of all the thermal events, we obtained the first derivative of the weight loss (Figure 9). Thermal transitions were divided

(32) Mutaftschiev, B. *The Atomistic Nature of Crystal Growth*; Series in Material Science; Springer-Verlag: Berlin, 2001; p 257.
(33) Kashchiev, D. *Nucleation Basic Theory with Applications*; Butterworth-Heinemann, Oxford, U.K., 2000; p 387.

in four steps: the first corresponds to the weight loss up to the point where a relative stability is achieved, around 150 °C; the second was set at ~150−280 °C; the third and fourth intervals were established at ~280−400 °C and ~400−820 °C, respectively. In the first temperature range, the samples lost between 10.5 and 13.4 wt %, depending on their chemical composition, which was assigned principally to hydration water (see the Supporting Information). At ~150−280 °C, the loss (1.7−3.5%) was attributed to removal of hydration water and physisorbed anions.[34] The third weight loss interval, where 18.7−24.4% was lost, corresponded to the dehydroxylation of the laminae and expulsion of the nitrate and carbonate anions located in the interlayer region in the form of CO_2 and NO_x.[35] Finally, in the fourth range, corresponding to the 7.5−10.6%, total dehydroxylation and expulsion of the remaining interlayer anions took place.

It is important to stress that during these thermal events, structural transformations take place. From the high-temperature powder X-ray diffraction of a MgAl-CO_3 LDH, it was found that in the first two ranges (up to 280 °C), the layered structure was maintained, and only an interlayer spacing decrease was noticed because of water and physisorbed anions removal. Around 360 °C, a structure collapse was appreciated, indicated by the absence of reflections in the X-ray pattern.[36] MgO crystallizes approximately at 400 °C, and at about 900 °C, a mixture of MgO-$MgAl_2O_4$ is obtained.[27] According to our results, and to those reported in the literature, the thermal decomposition and crystallographic transformations will depend mainly on the chemical composition of the LDH.[28,35]

Morphological Observations. Figure 10 (left side) presents the SEM images obtained at 2000x with the ESEM XL30, employing the signals generated by retrodispersed electrons. In general, it can be appreciated that the samples are homogeneous, due to their uniform contrasts, except for the MgCuAl sample where bright particles of ~800 nm can be observed. To verify these particles' chemical composition, an EDS analysis was performed. EDS at 400× revealed that the sample's molar ratio M^{2+}/M^{3+} was 2.36, which is close to the 2.73 determined by X-ray fluorescence. However, when a punctual analysis was carried out over the bright particles (see Figure 10), a copper enrichment molar ratio of 3.36 was noticed, resulting in a compositional contrast. This can be explained in terms of the known Jahn−Teller effect of the copper(II) ions[1] and their behavior in octahedral layers,[37] which could be enhanced by the mechanical dispersion.

The samples were also covered with gold and analyzed with the NOVA 200 SEM (Figure 10, right side). SEM

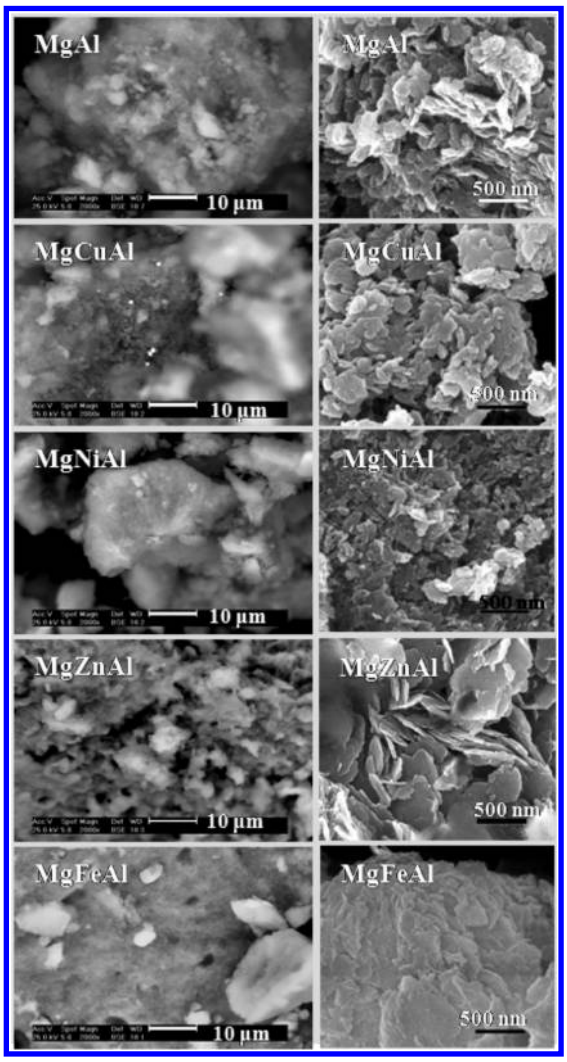

Figure 10. (Left) SEM images obtained from retrodispersed electrons of indicated samples. (Right) SEM images of the indicated samples covered with gold.

images showed that the LDHs consist of aggregates of flakelike particles, a morphology characteristic of LDHs.[38] The samples, depending on their chemical compositions, exhibited distinct average particle sizes being 64, 96, 103, 105, and 303 nm for the MgNiAl, MgAl, MgCuAl, MgFeAl, and MgZnAl, respectively, whereas the average thickness of the MgZnAl platelets (27 nm) could be calculated from their orientation. From the synthesis procedure, it was expected that mechanical dispersion would have a direct effect over the particle sizes, because dispersion transmitted energy to the system, favoring LDH crystallization. Therefore, similar particle sizes were expected in the MgCuAl and MgZnAl samples, which were dispersed for the same time (2 h); however, the differences were evident (103 and 303 nm, respectively).

As shown by the bright-field TEM images in Figure 11, different morphologies were developed depending on the chemical composition of the LDH.[8,39] For instance, MgAl sample consisted of nearly hexagonal-shaped

(34) Valente, J. S.; Cantú, M. S.; Cortez, J. G. H.; Montiel, R.; Bokhimi, X.; López-Salinas, E. *J. Phys. Chem. C* **2007**, *111*, 642.
(35) Chmielarz, L.; Kustrowski, P.; Rafalska, A.; Dziembaj, R. *Thermochim. Acta* **2005**, *395*, 225.
(36) Yang, W.; Kim, Y.; Liu, P. K. T.; Sahimi, M.; Tsotsis, T. T. *Chem. Eng. Sci.* **2002**, *57*, 2945.
(37) Yamaoka, T.; Abe, M.; Tsuji, M. *Mater. Res. Bull.* **1989**, *24*, 1183.
(38) Carja, G.; Nakamura, R.; Aida, T.; Niiyama, H. *Microporous Mesoporous Mater.* **2001**, *47*, 275.
(39) Perez-Ramirez, J.; Abelló, S.; van der Pers, N. M. *J. Phys. Chem. C* **2007**, *111*, 3642.

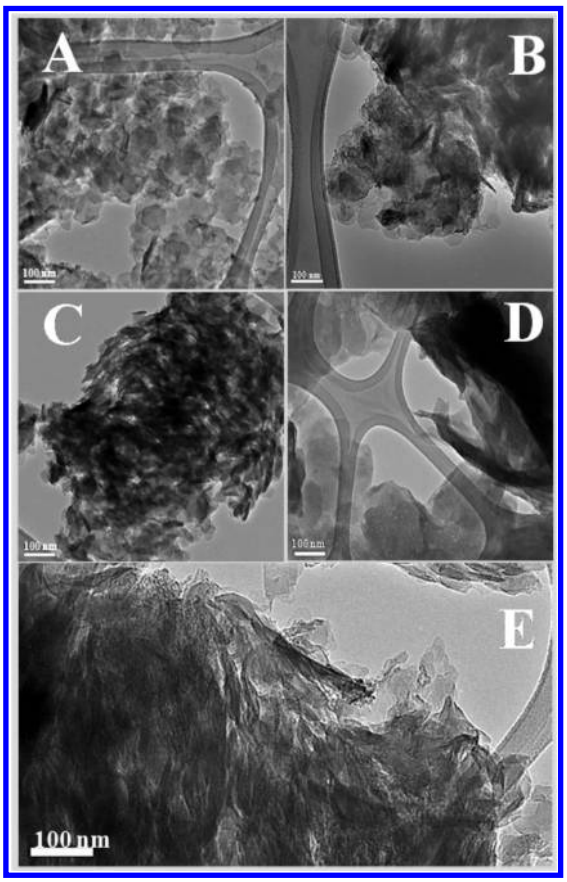

Figure 11. Bright-field TEM images: (A) MgAl, (B) MgCuAl, (C) MgNiAl, (D) MgZnAl, (E) MgFeAl.

nanoparticles, whereas MgCuAl, MgNiAl, MgZnAl, and MgFeAl are formed of ill-defined plate-shaped particles.

It is important to remark that the hexagonal morphology disclosed by the MgAl sample has been reported only for samples aged for long periods,[23,40] by hydrothermal[41] or microwave[42] treatments, whereas in this case, it was achieved at 80 °C for only 6 h under mechanical dispersion. The particle sizes calculated from the TEM measurements showed the same trend as those obtained from the SEM measurements, being MgNiAl < MgAl < MgFeAl ≈ MgCuAl, with average sizes of 65, 92, 98, and 101, respectively.

Textural Analysis. Specific surface areas, pore volumes, and average pore sizes of the fresh (outgassed at 100 °C) and calcined samples (outgassed at 350 °C) are summarized in Table 2. The samples outgassed at 100 °C presented specific surface areas between 32 and 93 $m^2\ g^{-1}$, very similar to those reported in the literature for samples prepared by coprecipitation.[43−46] Pore volumes oscillated between 0.137 and 0.445 for MgZnAl and MgAl, respectively.

The isotherm shape and the pore size distributions of the fresh and the calcined samples were similar in all the studied systems. Representative sample MgAl, outgassed at 100 and calcined at 500 °C, (Figure 12) displayed, in both cases, a type IV isotherm, which is characteristic of mesoporous materials.[47] Also, hysteresis loops over the relative pressure range 0.5−0.95 are type H3, attributed to aggregates of platelike particles leading to slit-shaped pores.[47] At low relative pressure, the absence of point B indicates that multilayer formation occurs from the beginning of the analysis. At relative pressures higher than 0.7, capillary condensation of the adsorbate in the meso−macropores takes place, giving a sharp adsorption volume increase. Isotherms and pore size distributions of the calcined, multimetallic samples can be found in the Supporting Information.

From the pore size distribution plots (insets in Figure 12), it can be observed that both the fresh and calcined sample showed broad bimodal pore size distributions in the meso and macropore range, between 20 and 60 and 100 to >1000 Å, correspondingly; their average values are stated in Table 2. For the multimetallic samples, outgassed at 100 °C, pore diameters in the first distribution were in the 36−92 Å range while the values of the second one lied between 243 and 424 Å. Furthermore, from the pore size distributions, it is meaningful to note that larger pores are predominant over the small ones, producing almost the total pore volume.

These differences can be explained by the different crystal sizes of the samples, which could lead to a different degree of stacking of the particles. In samples outgassed at 100 °C, porosity is due to interparticle voids, originated by the faulty stacking of platelets. Upon calcination, a topotactic transformation takes place; the interparticle porosity increases, attributed to a reorganization of the particles during calcination. Also, because of the expulsion of water and interlayer anions, a small, intraparticle porosity appears; this is known as the cratering effect.[46]

All the calcined samples (500 °C) show an increment in specific surface areas and pore volumes (Table 2), which is consistent with previous reports.[46] Conversely, an important decrease of pore size was noticed in the MgAl, MgNiAl, MgCuAl and MgZnAl calcined samples, when compared to the fresh samples. A plausible reason would be that during calcination, particles could be partially destroyed and particle size could be reduced. TEM analysis was performed over the MgAl sample, calcined at 500 °C for 4 h, in order to probe the proposed hypothesis. The sample was first calcined, grinded and deposited on a Holey copper grid coated with a carbon film.

(40) Liu, Z.; Ma, R.; Ebina, Y.; Iyi, N.; Takada, K.; Sasaki, T. *Langmuir* **2007**, *23*, 861.
(41) Rao, M. M.; Reddy, B. R.; Jayalakshmi, M.; Jaya, V. S.; Shridar, B. *Mater. Res. Bull.* **2005**, *40*, 347.
(42) Benito, P.; Labajos, F. M.; Rives, V. *Cryst. Growth Des.* **2006**, *6*, 1961.
(43) Trombetta, M.; Ramis, G.; Busca, G.; Montanari, B.; Vaccari, A. *Langmuir* **1997**, *13*, 4628.
(44) Holgado, M. J.; Rives, V.; San Román, M. S. *Appl. Catal., A* **2001**, *214*, 219.
(45) Ohishi, Y.; Kawabata, T.; Shishido, T.; Takaki, K.; Zhang, Q.; Wang, Y.; Nomura, K.; Takehira, K. *Appl. Catal., A* **2005**, *288*, 220.
(46) Reichle, W. T.; Kang, S. Y.; Everhardt, D. S. *J. Catal.* **1986**, *101*, 352.
(47) Rouquerol, F.; Rouquerol, J.; Sing, K. *Adsorption by Powders and Porous Solids*; Academic Press, London, 1999; Chapter 7, pp 204−212.

Table 2. Textural Analysis of the Solids at 100 and 500 °C

	specific surface area ($m^2\ g^{-1}$)		total pore volume ($cm^3\ g^{-1}$)		average pore diameter (Å)			
					100 °C		500 °C	
sample	100 °C	500 °C	100 °C	500 °C	I	II	I	II
MgAl	93	227	0.445	0.987	36	422	49	345
MgCuAl	50	230	0.281	0.882	39	424	56	343
MgNiAl	63	223	0.377	0.852	40	324	61	330
MgZnAl	32	140	0.137	0.428	92	411	34	345
MgFeAl	47	145	0.234	0.495	64	243	65	336

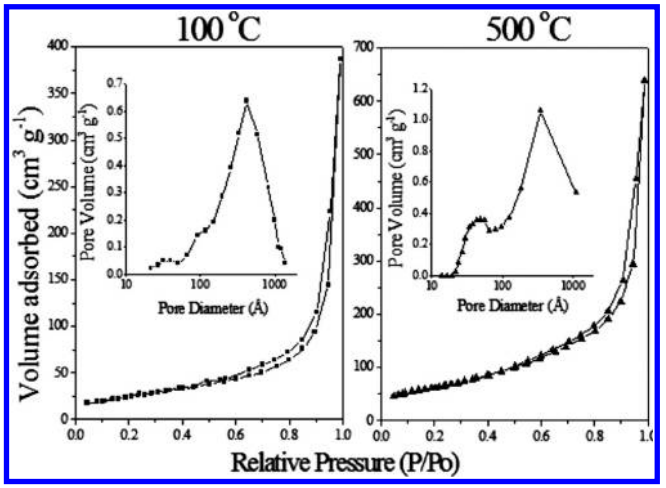

Figure 12. Comparative adsorption−desorption isotherms of the MgAl LDH treated at 100 and 500 °C. Inset: corresponding pore size distributions.

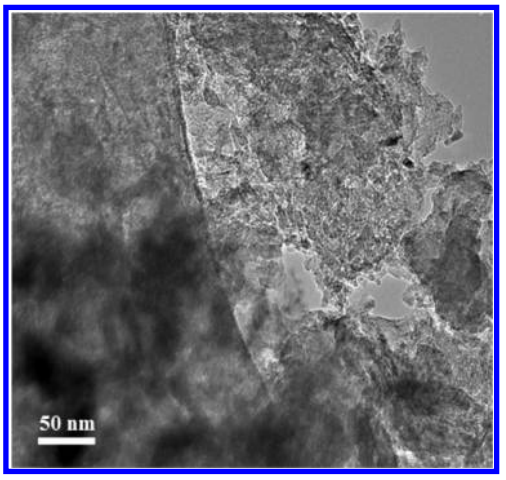

Figure 13. Bright-field electron microscopy image of the sample MgAl calcined at 500 °C.

No dispersion media, such as water or alcohol, were used, to avoid the structural reconstruction due to the known memory effect of LDHs.[1] According to the bright-field TEM image of the calcined MgAl (Figure 13), it can be appreciated that the hexagonal morphology displayed by the fresh sample was completely lost, giving rise to ill-defined platelike particles, whose size could not be determined due to their aggregation state. Though, at least in a qualitative sense, these particles are smaller than those found in the fresh sample. According to this result, it can be concluded that the observed pore size decrease corresponds to a particle size diminution caused by the solid's calcination.

Conclusions

LDHs were obtained by an economical method that does not require use of highly corrosive raw materials, prolonged hydrothermal treatments for crystallization, and more importantly, washing or purifying of the final product. The fundamental parameters in this procedure have been elucidated. A dissolution−precipitation−recrystallization mechanism was proposed and supported by experimental evidence. Furthermore, the preparation of composite materials with a Mg-enriched core and an outer shell rich in Al can be achieved by modifying synthesis times. Pure LDH phase is obtained after aging for only 6−8 h; large particles with uniform size were observed by SEM. Surface areas ranged from 32 to 93 $m^2\ g^{-1}$ and from 140 to 230 $m^2\ g^{-1}$ for fresh and calcined samples, respectively. Therefore, both LDHs and their calcination products have very similar properties to those prepared by conventional coprecipitation or urea hydrolysis procedures. This new method is intended to satisfy the growing demand of LDHs in large-scale applications as catalysts, SO_x adsorbents, PVC additives, etc.

Acknowledgment. This work was financially supported by the Instituto Mexicano del Petroleo. Authors thank J. F. Jaramillo and G. Cedillo for providing technical support.

Supporting Information Available: Detailed material synthesis procedure, average particle sizes after mechanical dispersion, line width of ^{27}Al MAS NMR signal of sample MgAl at different times after starting the synthesis, TGA weight loss intervals and amounts, XRD patterns of boehmite and BANS gel, and textural analyses of calcined multimetallic LDHs (PDF). This material is available free of charge via the Internet at http://pubs.acs.org.